Bioorganic & Medicinal Chemistry 16 (2008) 8619–8626

Contents lists available at ScienceDirect

Bioorganic & Medicinal Chemistry

journal homepage: www.elsevier.com/locate/bmc

Development and biological evaluation of C_{60} fulleropyrrolidine-thalidomide dyad as a new anti-inflammation agent

Sheng-Tung Huang [a,*], Chia-Shin Ho [b], Chun-Mao Lin [c], Hsu-Wei Fang [b], Yi-Xiang Peng [b]

[a] Graduate Institute of Biotechnology, National Taipei University of Technology, 1, Sec. 3, Chung-Hsiao E. Road, Taipei 106, Taiwan
[b] Graduate Institute of Chemical Engineering, National Taipei University of Technology, Taipei, Taiwan
[c] College of Medicine, Taipei Medical University, Taipei, Taiwan

ARTICLE INFO

Article history:
Received 25 June 2008
Revised 1 August 2008
Accepted 2 August 2008
Available online 7 August 2008

Keywords:
Anti-inflammation
C_{60} fulleropyrrolidine
TNF-α
Nitric oxide
Thalidomide

ABSTRACT

Research studies in the field of C_{60} fullerene derivatives have significantly increased due to the broad range of biological activities that were found for these compounds. We designed and prepared a new C_{60} fullerene hybrid bearing thalidomide as a potential double-action anti-inflammatory agent, capable of simultaneous inhibition of LPS-induced NO and TNF-α production. The C_{60} fulleropyrrolidine-thalidomide dyad, CLT, was an effective agent to suppress the release of NO and TNF-α by the LPS-stimulated macrophages RAW 264.7. Ten micromolars of CLT effectively inhibited LPS-induced NO and TNF-α production by 47.3 ± 4.2% and 70.2 ± 4% with respected to the control, respectively. Furthermore, preliminary biochemical investigation revealed that CLT was a potent agent to suppress both LPS-induced intracellular ROS production and iNOS expression, and CLT also inhibited the phosphorylation of ERK which is an important protein kinase involved in the activation of TNF-α synthesis in LPS-activated macrophages. We believed that the studies herein would hold promise for future development of a new generation of potent anti-inflammatory agents.

1. Introduction

Inflammation is a complex cellular event, in which parts of the event involve the secretion of various cytokines by immune cells. The two pro-inflammatory cytokines, nitric oxide (NO) and tumor necrosis factor α (TNF-α), have been recognized as essential components in acute and chronic inflammatory processes.[1] NO is associated with dilating the arteries and increasing the blood flow during inflammation. The pro-inflammatory enzyme, inducible forms of nitric oxide synthase (iNOS), is responsible for increasing the levels of NO, and it is highly expressed in lipopolysaccharide (LPS)-activated macrophages.[2] The polypeptide cytokine, TNF-α, is produced by cells of the monocyte/macrophage lineage. The process of TNF-α production starts with the binding of microbial products to cell surface Toll receptors, which results in initiating a cascade of signal transduction events which lead to activation of its synthesis.[1b] Both NO and TNF-α serve to recruit other inflammatory cells, which in turn release more cytokines and subsequently amplify the immune response. The cytokine responses to cell injury are regulated processes and are usually beneficial to the hosts, but overexpression of these cytokines can cause serious diseases including rheumatoid arthritis, multiple sclerosis, asthma, and psoriasis.

Research studies in the field of C_{60} fullerene derivatives have significantly increased due to the broad range of biological activities that were found for these compounds.[3] Recently, the preparation of novel water soluble fullerene hybrids bearing a variety of functional moieties such as peptides,[4] oligonucleotides,[5] porphyrins,[6] and flavonoids[7] have attracted much attention. Such dyad systems could amplify or alter the biochemical characteristics of their components or even produce compounds with new biological properties. In addition, the peculiar structure of C_{60} fullerene which is capable of 'adding' multiple radicals per molecule can serve as a 'radical sponge'.[8] The exceptional radical scavenging property of fullerene makes it a promising pharmacophore to target diseases caused by the overexpression of radicals.

Current therapeutic approaches to the treatment of inflammatory diseases are centered on the suppression of the NO and TNF-α production.[9] Oxidative stress by oxygen radicals is known to induce cellular instability by cascade events leading to inflammation, and it has been reported that suppression of ROS-mediated NO elevation is beneficial in reducing the development of inflammation.[10] Inhibiting the TNF-α production through suppressing the expression of inflammation-activated protein kinases had always been a hopeful target for the rational development of anti-inflammatory drugs.[1b] As part of the program aimed at discovering new anti-inflammation agents,[11] we had designed and prepared several C_{60} fullerene-anti-TNF-α dyads which simultaneously inhibited the NO and TNF-α production during inflammation. Several studies have revealed that C_{60} fullerene derivatives exhibit potent inhibitory effects on NO-dependent relaxation, and the inhibitory effects are believed to be associated with C_{60} fullerene radical scavenging

* Corresponding author. Tel.: +886 02 2771 2171; fax: +886 02 2731 7117.
E-mail address: Ws75624@ntut.edu.tw (S.-T. Huang).

0968-0896/$ - see front matter © 2008 Elsevier Ltd. All rights reserved.
doi:10.1016/j.bmc.2008.08.004

and direct NO-quenching abilities.[8,12] We expected that the exceptional radical scavenging activity and direct NO-quenching abilities of C_{60} fullerene would be beneficial to suppress the ROS-mediated NO elevation during inflammation. However, our previous results had shown that water soluble C_{60} derivatives alone lacked the efficacy to suppress the TNF-α production in the LPS-activated macrophage.[11] By covalently linking a known anti-TNF-α production agent to the C_{60} fullerene moiety, the new C_{60} fulleropyrrolidine-anti-TNF-α agent dyad expressed potent synergistic anti-inflammatory effects that inhibited both the NO and TNF-α production in LPS-activated macrophages at low micro molar concentration.[11]

Based on our previous results, we explored the modularity of our previous design, probing its applicability to incorporate another anti-TNF-α pharmacophore. We synthesized a new C_{60} fullerene hybrid bearing thalidomide (CLT) as a new anti-inflammation agent (Scheme 1). Thalidomide is a hypnotic/sedative drug that was withdrawn from the market because of its severe teratogenicity.[13] In spite of this, research into thalidomide was not halted, and thalidomide has been established as a potent immunomodulator with biological effects on both cytokine stimulation and cell-mediated immunity.[13] The basic chemical architecture of CLT is composed of thalidomide linked to the nitrogen of a C_{60} fulleropyrrolidine moiety through ethylene glycol chains, and an additional polar side chain was strategically positioned on the fullerene spheroid of the dyad to provide the extra hydration sites in order to enhance its solubility in aqueous media (Scheme 1). In this paper, we describe the synthesis of CLT, and we evaluate its anti-inflammatory effects by determining the amount of LPS-induced NO and TNF-α released by the macrophages RAW 264.7. We also investigated the mechanism of CLT in suppressing NO production by examining its abilities to modulate the intracellular ROS accumulation and the expression of iNOS in LPS-activated macrophages. Furthermore, mitogen-activated protein kinase (MAPK), an extracellular signal-regulated kinase (ERK), is an important inflammation-activated protein kinase which is involved in the cascade of TNF-α synthesis. Dmuitru et al. revealed that abolishing ERK activation by LPS inhibited the induction of TNF-α release, and further investigation revealed that the inhibition of ERK phosphorylation prevented the transport of TNF-α mRNA from the nucleus to the cytoplasm during inflammation.[14] The influence of CLT on modulating the phosphorylation of ERK had also been studied in LPS-activated macrophages by Western blot.

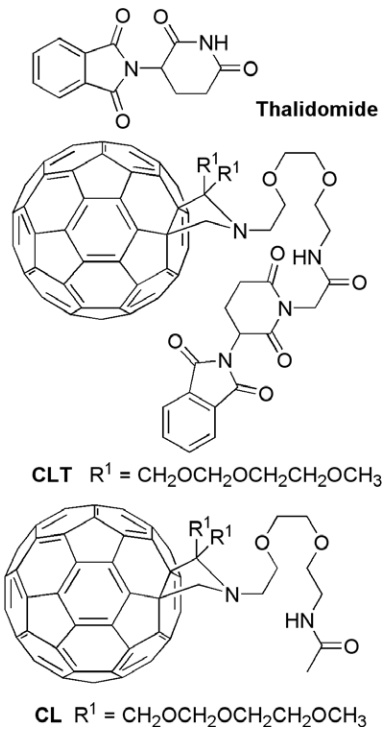

Scheme 1. Chemical structure of thalidomide, CLT, and CL.

2. Results and discussion

2.1. CLT synthesis and aqueous solubility

The synthetic scheme of CLT is outlined in Scheme 2. The synthesis began with the preparation of *N*-alkyated glycine **3**. Coupling the known acid **1**[15] with an amine salt **3**[16] under standard peptide coupling conditions gave the corresponding amide. Removing two benzyl protecting groups in the corresponding amide by a palladium-catalyzed hydrogenation reaction furnished the *N*-alkyated glycine **3** in 2 steps in 64% yield. The fulleropyrrolidine moiety in CLT was constructed by 1–3 dipolar cycloaddition reactions. Condensing the *N*-alkyated glycine **3** with known di-methoxyethoxymethyl-protected-ketone **4**[17] formed the corresponding azomethine ylide (not shown) which underwent 1–3 dipolar cycloaddition reactions with C_{60} fullerene to yield the desired fulleropyrrolidine-thalidomide dyad, CLT, and the yield was 25%. CLT was soluble in 1% DMSO aqueous solution with a maximum concentration of 1.16×10^{-5} M. The UV–vis spectra of CLT in 1% DMSO aqueous solutions showed that the main absorption of the fullerene core was still evident, although in analogy to other fullerene derivatives dissolved in polar solvents, the bands are broader and less structured, especially in the low-energy region (Supplementary materials). Amphiphilic fullerene monomers are known to form a colloidal in aqueous solutions;[18] we also examined the size distribution of CLT in the 1% DMSO aqueous solution. The intensity size distribution of CLT was measured by a dynamic light scattering (DLS) particle size analyzer (Supplementary materials). The average hydrodynamic diameter for 10 μM of CLT was 78.9 nm, and this value is similar to other known water soluble fullerenes measured in aqueous media.[18] Recently, there have been several papers describing the preparation of novel fulleropyrrolidine hybrids bearing promising biological components, but their best solubility in a 10% DMSO aqueous solution was reported to be in the range of $\sim 10^{-5}$ M,[7] and this presents a challenge the further evaluation in a mammalian cell culture model. The concentration of DMSO exceeding 1% in cell media caused instability of mammalian cells during culturing and biological evaluation. The synthesis of the CLT was completed in 3 steps from the known starting materials, and it is soluble in 1% DMSO aqueous solution in which it is suitable for evaluation with a mammalian culture model.

2.2. CLT cytotoxicity

We first analyzed the cytotoxic effects of CLT and its thalidomide-lacking structural analogues CL (Scheme 1) against a RAW 264.7 cell culture lineage via MTT assay; the cell viability results are shown in the Supplementary materials. Cytotoxicity studies after 24 h of continuous exposure to the various concentrations of CLT and CL with or without LPS stimulation were measured with a colorimetric assay based on the ability of mitochondria in viable cells to reduce MTT as described previously.[19] The RAW 264.7 cells pretreated with 10 μM of either CLT or CL in the presence of 1 μg/ml of LPS for 24 h had viability close to 95% with respect to the control. One interesting observation was that we observed a slight increase in the cells' viability when the RAW 264.7 culture was incubated with 10 μM of CLT without LPS stimulation. CLT and CL were not cytotoxic to the RAW 264.7 cell culture lineage.

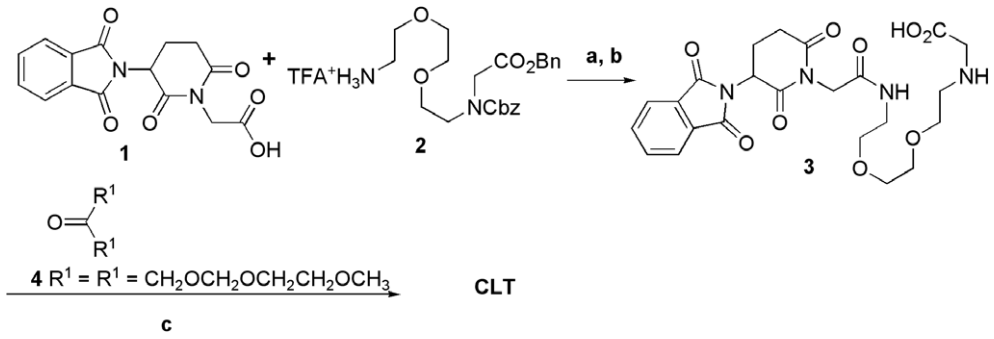

Scheme 2. Reagents and conditions: (a) EDCI, HOBT, Et_3N, DMF, rt, 16 h, 70%; (b) H_2 (60 psi), Pd/C, 18 h, 91%; (c) toluene, reflux, 25%.

2.3. CLT anti-inflammatory evaluation

We evaluated the anti-inflammatory effects of thalidomide, CL, an equimolar concentration of thalidomide–CL cocktail, and CLT on the LPS-activated macrophages RAW 264.7 by determining the amount of NO and TNF-α released into the cell supernatants. The RAW 264.7 cells were pretreated with thalidomide, CL, an equimolar concentration of thalidomide–CL cocktail, or CLT at different concentrations (10, 1, and 0.1 μM) for 3 h, followed by stimulating the cells with LPS (1 μg/mL) for 24 h. RAW 264.7 stimulated with LPS alone was the control. The amount of NO was determined by measuring the nitrite concentrations in the cell supernatants after 24 h treatment.[20] The concentration of TNF-α was determined by the ELISA method as described according to the known prior art.[21] The results are shown in Figures 1 and 2. All tested herein agents showed an inhibitory effect on LPS-induced NO production in a concentration-dependent manner (Fig. 1). The RAW 264.1 pretreated with 10 μM of either the CL or the thalidomide–CL cocktail exhibited a moderate reduction of NO synthesis, and the concentrations of NO produced were 32.3 ± 1.6 and 35.7 ± 3.1 μM, respectively, and those values were 30.9 ± 3.5% and 23.7 ± 6.7% reduction with respect to the control. In contrast, thalidomide and CLT were potent agents to reduce the LPS-induced NO secreted by the macrophages. The concentrations of NO detected in the cell supernatants were 26.9 ± 2.5 and 25.2 ± 1.9 μM for cells pretreated with 10 μM of thalidomide and CLT, respectively, and those values were 44.1 ± 5.8% and 47.3 ± 4.2% reduction with respect to the control. All agents tested herein had no quenching effect on the Griess reagent at the concentrations used. On the other hand, the macrophages pretreated with either thalidomide, thalidomide–CL cocktail or CLT exhibited a significant reduction in the TNF-α synthesis. RAW 264.7 pretreated with 10 μM of either thalidomide or thalidomide–CL cocktail exhibited a reduction in TNF-α, and the concentrations of TNF-α detected in the cell medium were 9.2 ± 0.8 and 11.9 ± 1.7 ng/ml, respectively, and those values were 55.5 ± 3.6% and 41.9 ± 8% reduction with respect to the control (Fig. 2). CLT exhibited an impressive effect on suppressing the LPS-induced TNF-α synthesis at either 1 or 10 μM in the pretreatments; the concentrations of TNF-α detected in the cells medium were 11.5 ± 1.5 and 5.3 ± 1.0 ng/ml, respectively, and those values were 44.4 ± 7.2% and 70.2 ± 4% reduction with respect to the control. The non-covalently-linked thalidomide CL cocktail is less effective in reducing the LPS-induced NO and TNF-α production compared to the fulleropyrrolidine-thalidomide dyad, CLT. Furthermore, CLT is nearly tenfold more potent than thalidomide alone in suppressing the LPS-induced TNF-α production by the macrophages. CLT is the most potent agent herein tested in suppressing NO and TNF-α synthesis in the LPS-activated macrophages.

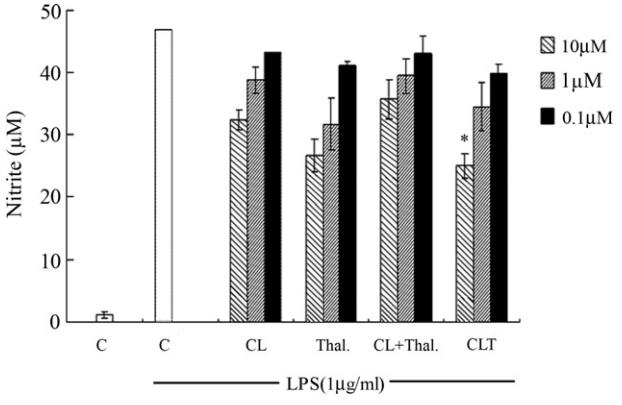

Figure 1. Nitrite production in RAW 264.7 cells pretreated with the indicated concentration of CL, Thal (thalidomide), CL + Thal (an equimolar thalidomide–CL cocktail), and CLT for 3 h. The cells were activated with LPS (1 μg/ml). Control cells were incubated with DMSO alone. Culture supernatants were collected after a 24-h activation. Error bars represent the standard error of mean ($n = 3$). Significant difference ($P < 0.01$) compared with the control treated with LPS.

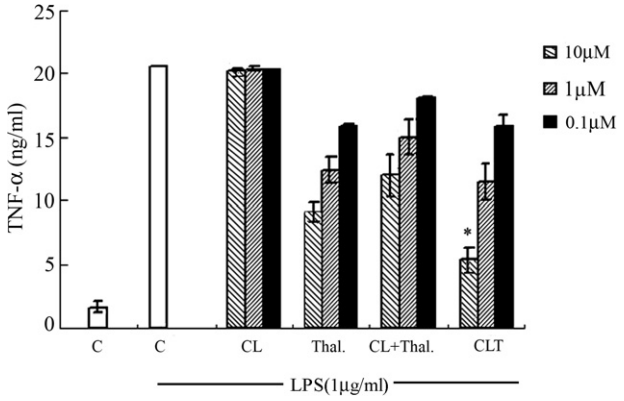

Figure 2. TNF-α production in RAW 264.7 cells pretreated with the indicated concentration of CL, Thal (thalidomide), CL + Thal (an equimolar thalidomide–CL cocktail), and CLT for 3 h. The cells were activated with LPS (1 μg/ml). Control cells were incubated with 1% DMSO alone. Culture supernatants were collected after 24-h activation. Error bars represent the standard error of mean ($n = 3$). Significant difference ($P < 0.01$) compared with the control treated with LPS.

2.4. The scavenging effect of thalidomide, CL, and CLT to ROS

Intracellular ROS is an important signal mediator in the inflammation process, and its concentration elevates during inflammation. We evaluated the influence of thalidomide, CL, an equimolar concentration of thalidomide–CL cocktail, and CLT on modulating intracellular ROS concentration in the LPS-activated macrophages RAW 264.7. The formation of intracellular ROS was visualized by

confocal microscopy a with latent fluorescent probe, DHR 123, whose its intense fluorescent rhodamine could be selectively revealed by the ROS oxidation, and the results are shown in Figure 3.[22] The RAW 264.7 cells were pretreated with 10 μM of either CLT, CL, thalidomide, or an equimolar concentration of thalidomide–CL cocktail followed by stimulating them with LPS (1 μg/mL) for 3 h. The RAW 264.7 stimulated with LPS alone was the control. The RAW 264.7 stimulated with LPS alone exhibited an intense fluorescent signal (Fig. 3b). In contrast, the cells pretreated with all of the agents herein tested resulted in the diminished intensity of the fluorescent signal within cells via visualizing this through a confocal microscope (Fig. 3c–f). Flow cytometric detection of intracellular ROS was also preformed by examining the oxidation of green DHR 123 fluorescence by ROS in the LPS-stimulated RAW 264.7 cells (Fig. 4). Once again, the cells pretreated with all of the agents herein tested showed inhibition of the ROS-associated green DHR 123 fluorescence, and these results were consistent with the results of confocal microscopy (Fig. 4c–f). The cells pretreated with thalidomide or CLT exhibited the weakest fluorescent signal compared to other agents herein tested (Fig. 4d and f). Because radical scavenging by C_{60} fullerene has been widely demonstrated in vitro, interestingly it was noted that CL alone also exhibited a potent effect on reduction of the intensity of the DHR 123 fluorescent signal (Figs. 3c and 4c). The results of the above experiments indicated that all of the reagents tested herein were effective in decreasing the accumulation of intracellular ROS concentration in the LPS-activated RAW 264.7

2.5. The influence of thalidomide, CL, and CLT on iNOS expression

The pro-inflammatory enzyme, iNOS, is responsible for increasing the levels of NO, and it is highly expressed in lipopolysaccharide (LPS)-activated macrophages.[2] We examined the expression of iNOS in RAW 264.7 cells pretreated with the agents tested herein after LPS stimulation, and the Western blot results are shown in Figure 5. The macrophages stimulated with LPS alone after 24 h exhibited a large expression of iNOS (Fig. 5, lane 2). The iNOS expression in the LPS-activated macrophages pretreated with either 1 or 10 μM of thalidomide or CLT had a minimum or essentially no expression of iNOS protein (Fig. 5, lanes 5, 6, 9, and 10). On the other hand, the cells pretreated with an equimolar concentration of thalidomide–CL cocktail (10 μM) exhibited a moderate iNOS expression. Interestingly, cells pretreated with CL (10 μM) also exhibited a minor reduction of the expression of iNOS after LPS stimulation. CLT and thalidomide were the most potent agents tested herein on reducing the expression of iNOS.

Suppression of the ROS-mediated NO released by macrophages through scavenging intracellular ROS has been widely demonstrated in vitro. The chemical structure of CL contains a 'radical sponge' C_{60} fullerene moiety which exhibited a potent effect on reducing the intracellular ROS concentration; thus, it suppressed the LPS-induced NO production by the macrophages. However, CL lacked efficacy in suppressing iNOS expression. From this study, we observed that the C_{60} fullerene hybrid with an iNOS expression suppressing agent, thalidomide, dyad (CLT), exhibited a synergistic effect on suppressing the NO production; macrophages pretreated with CLT were more potent in reducing the NO production compared to CL pretreatment alone. Unfortunately, we did not observe much improvement in the efficacy of inhibiting NO production compared between cells pretreated with either CLT or thalidomide alone. The chemical structure of CLT contains both a 'radical sponge' and an iNOS suppressing agent exhibiting potent synergistic anti-inflammatory effects that inhibited the LPS-induced NO synthesis by the macrophages. CLT inhibition of NO synthesis by the LPS-stimulated macrophages is attributed to its abilities to scavenge intracellular ROS and suppress the iNOS expression.

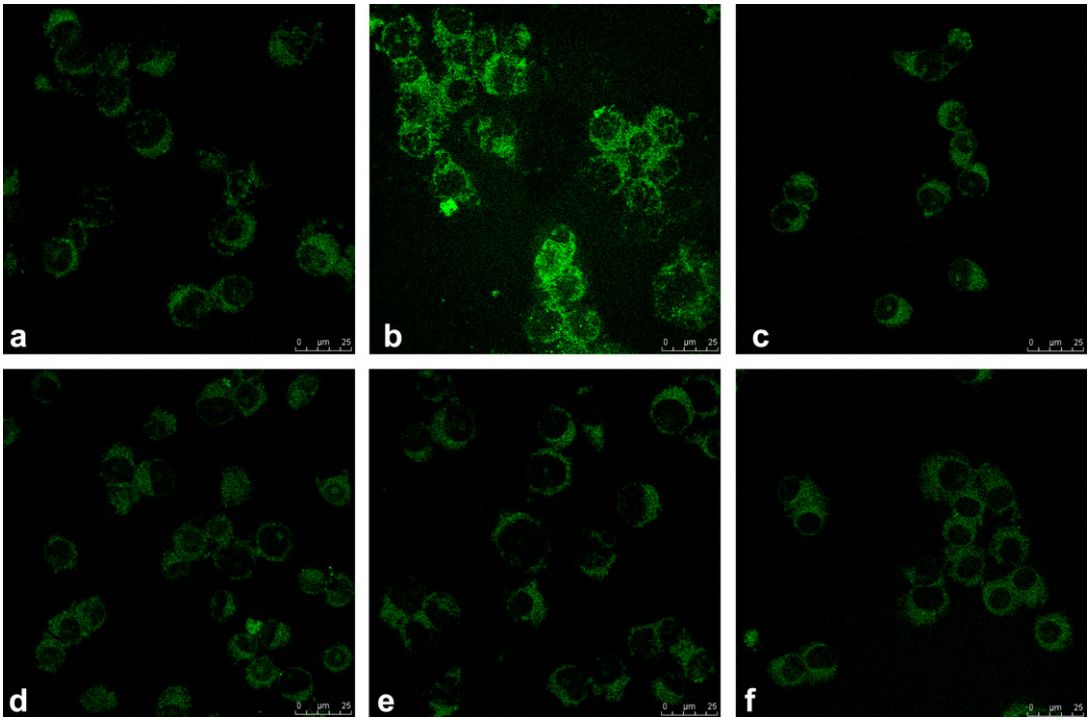

Figure 3. The intracellular reactive oxygen species (ROS) production in RAW 264.7 cells visualized with the oxidized DHR123 green fluorescence through confocal a microscope. Confocal images of green oxidized DHR123 fluorescence in the RAW 264.7 cells with (a) alone, (b) 1-h LPS (100 ng/ml) stimulation alone, (c) CL (10 μM) 3-h pretreatment, (d) thalidomide (10 μM) 3-h pretreatment, (e) an equimolar thalidomide–CL cocktail (10 μM) 3-h pretreatment, or (f) CLT (10 μM) 3-h pretreatment, followed by 1-h LPS (100 ng/ml) stimulation and stained with 10 μM of DHR123 for 30 min.

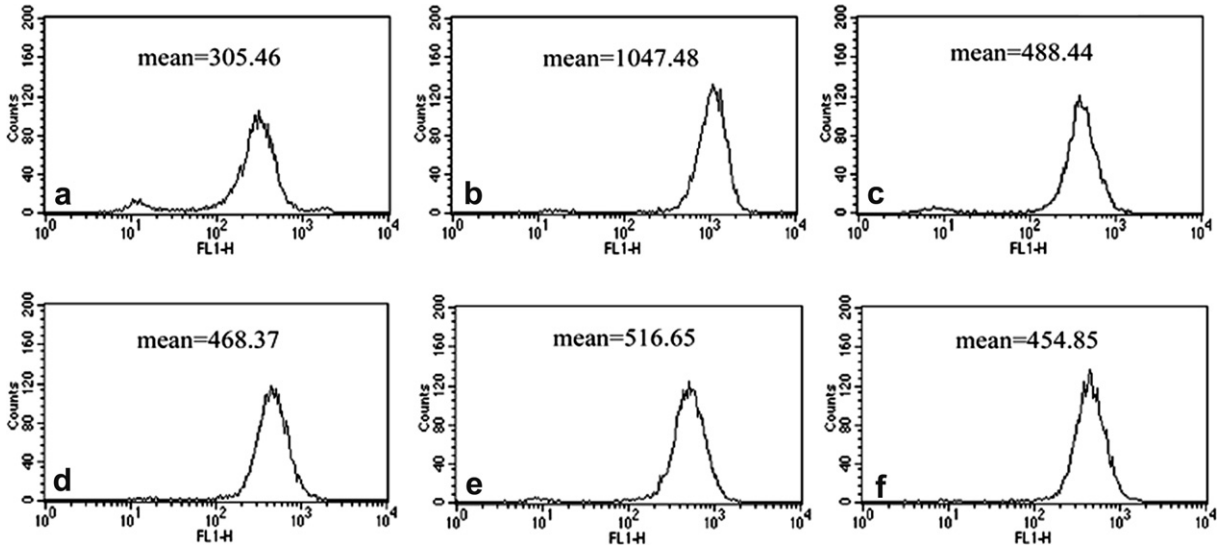

Figure 4. The intracellular reactive oxygen species (ROS) production in RAW 264.7 cells measured by the green fluorescence of oxidized DHR123 through a flow cytometer. The FL1-H fluorescence intensity, represented by mean values, on a FACScan flow cytometer was evaluated for LPS stimulation (100 ng/ml) for 30 min. Flow cytometer spectra of green oxidized DHR123 fluorescence in the RAW 264.7 cells with (a) alone, (b) 1-h LPS stimulation alone, (c) CL (10 μM) 3-h pretreatment, (d) thalidomide (10 μM) 3-h pretreatment, (e) an equimolar thalidomide–CL cocktail (10 μM) 3-h pretreatment, or (f) CLT (10 μM) 3-h pretreatment.

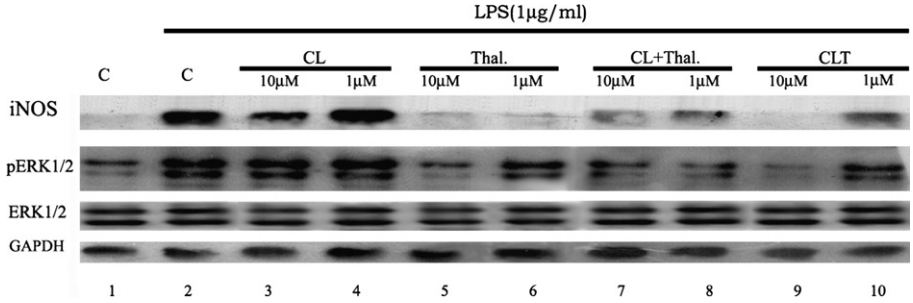

Figure 5. The expression of iNOS and pERK was assessed by immunoblot. The RAW 264.7 cells pretreated with various concentrations (1 and 10 μM) of CL, Thal (thalidomide), CL + Thal (an equimolar thalidomide–CL cocktail), and CLT for 3 h followed by LPS (1 μg/ml) stimulation, and cell lysate prepared for analysis. Lane 1, shows is the untreated cell control, and lane 2, shows is the cells with LPS stimulation alone. The immunoblots shown have been equilibrated for protein loading. The data shown are representative of three separate experiments.

2.6. The influence of thalidomide, CL, and CLT on ERK phosphorylation

Finally, ERK is an important inflammation-activated protein kinase which is involved in the cascade of TNF-α synthesis. The phosphorylated ERK (pERK) was known to be involved in the translocation of the TNF-α mRNA from the nucleus to the cytoplasm. We also looked into the expression of pERK 1 and 2 in RAW 264.7 cell pretreated with the agents here in tested after LPS stimulation for 30 min, and the Western blot results are also shown in Figure 5. The macrophages stimulated with LPS alone for 30 min exhibited a large amount of pERK 1 and 2 expressions (Fig. 5, lane 2). In contrast, cells pretreated with either thalidomide or CLT after LPS stimulation exhibited minimum amount of pERK 1 and 2 expressions compared to LPS-stimulated cells alone (Fig. 5, lanes 5, 6, 9, and 10). The cells pretreated with 10 μM of CLT exhibited the lowest expressions of pERK 1 and 2 compared to the other agents herein tested (Fig. 5, lane 9). However, cells pretreated with an equimolar concentration of thalidomide–CL cocktail (10 μM) and CL alone (10 μM) exhibited only moderate or no inhibitory effects on pERK expression after LPS stimulation. CLT is the most potent of the agents tested herein in suppressing the pERK expression in the LPS-activated macrophages.

The biochemical mechanism of thalidomide-inhibited TNF-α production in the LPS-activated macrophages had been studied. Many studies had demonstrated that thalidomide inhibited TNF-α production through suppressing p-38 expression thus destabilizing the TNF-α mRNA for translation.[13] However, thalidomide suppression of pERK expression in the LPS-activated macrophages RAW264.7 has not been documented. Our preliminary biochemical mechanism study of both thalidomide and CLT on inhibiting LPS-induced TNF-α production revealed that they both inhibited the TNF-α synthesis through suppressing the pERK expression. Furthermore, the C_{60} fullerene moiety alone was unable to modulate the activation of ERK, and CLT containing the bulky C_{60} fullerene moiety did not hamper the effect of thalidomide on suppressing pERK expression. Further details of molecular pharmacological studies involving CLT on modulating the activity of other kinases in the cascade of the TNF-α synthesis are underway.

From this study, we observed different efficacies between CLT and the thalidomide–CL cocktail treatment on LPS-induced macrophages. Although the thalidomide–CL cocktail contains both pharmacophores as does CLT, the thalidomide–CL cocktail treatment is far less effective in suppressing LPS-induced NO and TNF-α synthesis, iNOS and pERK expression compared to CLT treatment alone. LPS-stimulated macrophages pretreated with CLT (10 μM) exhibited 47.3 ± 4.2% and 70.2 ± 4% reduction of NO and TNF-α production with respect to the control. However LPS-stimulated macrophages pretreated with thalidomide–CL cocktail (10 μM) only exhibited 23.7 ± 6.7% and 41.9 ± 8% reduction of NO and TNF-α production

with respect to the control. We postulated that the potent effect of CLT on reversing the inflammatory effects induced by LPS might be associated with the C_{60} fullerene moiety enhancing the delivery of the thalidomide into the cells. Yang et al. had demonstrated that the C_{60} fullerene moiety enhanced the delivery of amino acids into the cells.[23] In this study, we also observed similar effects in which the C_{60} fullerene moiety in CLT enhanced the delivery of the thalidomide moiety to cross the cell barriers; therefore, CLT was more effective in reversing the inflammatory effects induced by LPS. In contrast, the cocktail treatment does not assure equal delivery of both agents, and the thalidomide also lacks the enhancement of the delivery acted on by the C_{60} fullerene moiety. CLT is a C_{60} fullerene thalidomide dyad that amplifies the biochemical characteristics of thalidomide and produces a new biological property that exhibits potent synergistic anti-inflammatory effects.

3. Conclusion

We successfully prepared a new C_{60} fulleropyrrolidine-thalidomide dyad, CLT. Our biological evaluation using a cell lineage to simulate the type of macrophages present during inflammation had demonstrated that CLT was a potent agent in reducing both NO and TNF-α released into the cell medium. Furthermore, CLT inhibition of both NO and TNF-α synthesis in LPS-activated macrophages is attributed to its abilities to scavenge intracellular ROS, suppress the iNOS expression and inhibit ERK phosphorylation. We are currently exploring the utility of CLT on modulating other cytokines in the process of inflammation. We believed that the agents synthesized herein would hold promise for future development of a new generation of potent anti-inflammatory agents.

4. Experimental

4.1. General

All reactions were carried out under argon by using standard techniques. Solvent were dried under nitrogen by standard procedures, distilled before use, and store under argon. NMR spectra were recorded on a Bruker AMX-500 spectrometer. Chemical shifts were reported in ppm relative to tetramethylsilane (δ units). Fast atom bombardment (FAB) mass spectra and Electrospray ionization (ESI) at the Analytical Facility of The National Taiwan University. IR spectra were obtained on Perkin-Elmer Spectrum RXI FT-IR system. Chemicals were purchased from Acros, Aldrich, or TCI and used without future purification. CL was prepared according to our previous published procedure.[11] The RAW 264.7 cells were mouse macrophage cell line, and were obtained from American Type Culture Collection (ATCC, TIB-67). Fetal bovine serum (FBS) was purchased from Hyclone (Logan, UT, USA). Dulbecco's modified Eagle's medium (DMEM), penicillin, streptomycin, Lipopolysaccharide (LPS from *Escherichia coli* 026:B6) were purchased from Sigma (St. Louis, MO, USA). The stock solution of thalidomide, CL, and CLT prepared in DMSO and added to FBS before use, and the DMSO concentrations never exceeded 1% (v/v) in all the experiments. The enzyme-linked immunosorbent assay (ELISA) kit used for the determination of TNF-α was purchased from R&D systems (Minneapolis, MN, USA).

4.2. Synthetic procedures

4.2.1. (Benzyloxycarbonyl-{2-[2-(2-{2-[3-(1,3-dioxo-1,3-dihydro-isoindol-2-yl)-2,6-dioxo-piperidin-1-yl]-acetylamino}-ethoxy)-ethoxy]-ethyl}-amino)-acetic acid benzyl ester

Triethylamine (390 μL, 2.8 mmol) was added to a solution of acid **1** (1.13 g, 2.6 mmol) in 2 mL of DMF. In a separate flask, a solution of amine salt **3** (0.81 g, 2.9 mmol), EDCI (1.02 g, 5.3 mmol), and HOBT (0.75 g, 5.3 mmol) in 10 mL of DMF was stirred for 1 h and then added dropwise to the solution of **4** at room temperature. After 16 h, the solution was diluted with ethyl acetate (40 mL) and washed with acidic water (3 × 40 mL) and dried with $MgSO_4$, and the solvent was evaporated under reduced pressure. The crude material was purified by flash chromatography (eluent DCM/methanol, 95:5, R_f = 0.40) to afford the desired compound as an oil (1.39 g, 2.0 mmol, yield 77%). ^{1}H NMR (500 MHz, $CDCl_3$): δ = 2.12 (m, 1H), 2.82 (m, 2H), 2.95 (m, 1H) 3.40–3.61 (m, 12H), 4.18 (d, 2H, *J* = 20Hz), 4.42–4.52 (m, 2H), 5.08 (d, 2H, *J* = 14Hz), 5.12 (m, 1H), 5.16 (d, 2H, *J* = 5.1Hz), 6.52 (1H, NH), 7.24–7.34 (m, 10H), 7.73–7.74 (m, 2H), 7.85 (m, 2H). ^{13}C NMR (125 MHz, $CDCl_3$): 22.0, 31.5, 39.4, 42.9, 47.9, 48.5, 49.8, 50.3, 66.8, 67.4, 67.6, 69.7, 70.1, 123.7, 127.0, 127.7, 127.8, 127.9, 128.0, 128.1, 128.2, 128.3, 128.4, 128.5, 128.6, 131.7, 134.4, 135.4, 135.5, 136.3, 136.4, 156.0, 156.3, 166.5, 167.2, 168.4, 170.0, 170.6. FT-IR: $\nu\sim$ = 3363, 3064, 3034, 2950, 1681, 1614, 1499, 1457, 1240, 1172, 1135 cm^{-1}. MS (FAB+): *m/z* = 729 [M+1]. Calcd for $C_{38}H_{40}N_4O_{11}$, 728.

4.2.2. {2-[2-(2-{2-[3-(1,3-Dioxo-1,3-dihydro-isoindol-2-yl)-2,6-dioxo-piperidin-1-yl]-acetylamino}-ethoxy)-ethoxy]-ethylamino}-acetic acid (3)

A solution of above protected *N*-alkyated glycine (0.41 g, 0.6 mmol) in 10 mL of methanol was stirred for 18 h under hydrogen pressure (60 psi), with 10% Pd/C (0.04 g) as catalyst. The crude material was purified by filtration through Celite; the solvent was then evaporated under reduced pressure, yielding a solid (0.26 g, 0.6 mmol, yield 91%), ^{1}H NMR (500 MHz, D_2O): δ = 1.97 (s, 1H), 2.29 (m, 1H), 2.80 (m, 1H), 3.08 (m, 2H), 3.30 (t, 2H, *J* = 4.9 Hz), 3.47 (t, 2H, *J* = 4.9 Hz), 3.67–3.75 (m, 10H), 3.79–3.81 (t, 2H, *J* = 4.9 Hz), 4.53 (d, 1H, *J* = 16 Hz), 4.62 (d, 1H, *J* = 16 Hz), 5.39 (dd, 1H, *J* = 5.44 Hz, 13 Hz), 7.91–7.93 (m, 2H), 7.96–7.98 (m, 2H). ^{13}C NMR (125 MHz, $CDCl_3$): 21.4, 31.4, 39.4, 43.2, 47.2, 49.5, 50.2, 65.8, 69.2, 69.9, 70.0, 124.2, 131.4, 135.6, 169.5, 170, 171.5, 171.6, 174.4. FT-IR: $\nu\sim$ = 3452, 3426, 3416, 3072, 2961, 1769, 1721, 1687, 1559, 1494, 1468, 1457, 1173, 1130, 1102 cm^{-1}. MS(E-SI$^-$): *m/z* = 504 [M]. Calcd for $C_{23}H_{28}N_4O_9$, 504.

4.2.3. CLT

A mixture of C_{60} (0.05 g, 0.07 mmol), amino acid **3** (0.07 g, 0.14 mmol), and ketone **6** (0.35 mmol) in toluene (30 mL) was heated to reflux for 5 h. After evaporation of the solvent, the crude material was purified by flash chromatography. (DCM/methanol, 98:2, R_f = 0.39) Final product: 25 mg (25%) ^{1}H NMR (500 MHz, $CDCl_3$/*d*-acetone): δ = 2.81–2.84 (m, 2H), 2.98 (m,1H), 3.38 (s, 7H), 3.48–3.60 (m, 10H), 3.71–3.81 (m, 8H), 3.92 (m, 2H), 4.49–4.53 (m, 3H), 4.60 (d, 2H, *J* = 10 Hz), 4.82 (s, 4H), 4.88 (s, 2H), 5.11 (dd, 1H, *J* = 5.44 Hz, 13.02 Hz), 6.35 (br, 1H, NH), 7.74–7.77 (m, 2H), 7.86–7.88 (m, 2H). ^{13}C NMR (125 MHz, $CDCl_3$): 22.1, 29.7, 31.6, 39.5, 43.0, 53.3, 59.0, 67.1, 67.4, 67.5, 67.6, 67.8, 68.5, 69.7, 70.3, 70.7, 71.6, 71.7, 88.9, 92.6, 131.8, 134.4, 136.2, 141.8, 141.9, 142.1, 142.2, 142.6, 143.1, 145.3, 145.4, 145.7, 146.1, 146.2, 154.1, 155.0, 166.4, 167.2, 168.4, 170.5. MS (ESI+): *m/z* = 1430 [M+1]. Calcd. for $C_{93}H_{48}N_4O_{13}$, 1429.3952 Anal. Calcd for $C_{93}H_{48}N_4O_{13}$: C, 78.14; H, 3.38; N, 3.92. Found: C, 77.69; H, 3.35; N, 3.81.

4.3. Cell culture

The macrophage cell line RAW 264.7 was cultured in Dulbecco's modified Eagle's medium (DMEM) supplemented with 10% heat-inactivated fetal bovine serum (FBS), 100 U/ml penicillin, and 100 μg/ml streptomycin at 37 °C under 5% CO_2 humidified air.

4.4. Cell viability

The 3-(4,5-dimethyldiazol-2-yl)-2,5 diphenyl tetrazolium bromide (MTT) which could be reduced to yield formazone in cells'

mitochrondrial-dependent reduction was used as an indicator of cell viability. One day before drug application, the RAW 264.7 cells were seeded in 24-well flat-bottomed microtiter plates (2×10^5 cells/well). The RAW 264.7 cells were stimulated or not with LPS(1 μg/ml) alone or in combination with thalidomide, CL, CLT or an equimolar of thalidomide-CL cocktail (dissolved in DMSO). The final concentration of DMSO was 1% (v/v). The DMSO percentage allows the optimal solubilization of C_{60} fulleropyrrolidines in aqueous solutions. After 24 h of incubation at 37 °C, cells were washed with PBS once, and 0.2% MTT (100 μL) was added to the well for 3 h. Then, the supernatant was removed, and the formazone crystals were dissolved using DMSO. The optical density (OD_{570}) for the thalidomide, CL, CLT, or equal molar of CL and thalidomide cocktail mixture were compared to the OD of control or LPS(1 μg/ml)-stimulated wells to assess the cytotoxicity. The absorbance was read at 570 nm with an ELISA plate reader (TECAN Sunrise™, Switzerland). Data are report as mean ± SEM values of three independent determinations.

4.5. Nitrite assay

Nitric oxide (NO) production in cell culture supernatant was evaluated by measuring the nitrite concentration. The nitrite concentration was detected with the Griess reaction. The RAW 264.7 were plated at a density of 2×10^5 cells/ml in 24-well plates for 24 h, followed by treatment different concentrations of the indicated compounds, with thalidomide, CL, CLT, or an equimolar of thalidomide-CL cocktail for 3 h, then treatment with LPS (1 μg/ml) for 24 h. One hundred microliters of each supernatant was mixed with the same volume of Griess reagent (1% sulfanilamide in 5% phosphoric acid and 0.1% naphthylethylendiamine dihydrochloride in water) and incubated at room temperature for 10 min. The absorbance was read at 550 nm with an ELISA plate reader (TECAN Sunrise™, Switzerland). The amount of nitrite in the samples (in micromolar) was calculated from a sodium nitrite standard curve freshly prepared in culture medium. Data are report as mean ± SEM values of three independent determinations.

4.6. TNF-α assay

Soluble cytokine was tested in the supernatants of cultured RAW 264.7 macrophage by ELISA. The RAW 264.7 were plated at a density of 2×10^5 cells/ml in 24-well plates for 24 h, followed by treatment different concentrations of the indicated compounds such as with thalidomide, CL, CLT, or an equimolar of thalidomide-CL cocktail mixture for 3 h, then treatment with LPS (1 μg/ml) for 24 h. The TNF-α-protein in cell supernatant was detected using the ELISA kit (R&D, Catalogue No. DY410) and conducted according to the manufacturer instructions. The absorbance was read at 540 nm with an enzyme-linked immunosorbent assay (ELISA) plate reader (TECAN Sunrise™, Switzerland). Data are report as mean ± SEM values of three independent determinations.

4.7. ROS assay

Levels of cellular oxidative stress were measured using the fluorescent probe, dihydrorhodamine 123 (DHR123), as described previously. The DHR 123 dye enters mitochondria and fluoresces when oxidized by ROS. After treatment with 100 ng/ml LPS or pretreatment with CL (10 μM), thalidomide (10 μM), an equimolar thalidomide-CL cocktail (10 μM), or CLT (10 μM) for 3 h, cells were stained with 10 μM DHR123 for 30 min, and washed with phosphate-buffered saline. Cells were imaged using a confocal microscope (Leica TCS SP5, Bensheim, Germany). Cells were located under bright-field optics and then scanned once with a laser (with excitation at 488 nm and emission at 510 nm). Flow cytometric detection of intracellular ROS was performed as described previously.[19] RAW 264.7 cells were suspended in phenol red-free media at a concentration of 2×10^5 cells/ml. Cells were stained with 10 μM DHR123 in the dark for 30 min, and then analyzed using FACScan (Becton–Dickinson, Franklin Lakes, NJ). Oxidation of the green DHR123 fluorescence in living cells was detected using the FL1-H wavelength band. The fluorescence signals of 10,000 cells were processed using a logarithmic amplifier.

4.8. iNOS and ERK1/2 protein expression assay

The expressions of iNOS, ERK1/2 were detected by Western blot. After treatment with 1 μg/ml LPS or pretreatment with CL (10 μM), thalidomide (10 μM), an equimolar thalidomide-CL cocktail (10 μM), or CLT (10 μM) for 3 h, total cellular protein (for iNOS and ERK1/2) was prepared using lysis buffer containing 10% Glycerol, 1% Triton X-100, 1 mM sodium orthovanadate, 1 mM EGTA, 5 mM EDTA, 10 mM NaF, 1 mM sodium pyrophosphate, 20 mM Tris–HCl, pH 7.9, 100 mM B-glycerophosphate, 137 mM NaCl, 1 mM phenylmethylsulfonyl fluoride (PMSF), and 10 mg/ml aprotinin. Thirty to fifty milligrams of proteins were separated on sodium dodecyl sulfate–polyacrylamide gel (SDS–PAGE) (10% for iNOS, phospho-ERK1/2, ERK1/2, and GAPDH) and electro transferred to polyvinylidene difluoride (PVDF) membrane (ImmobilonP, Millipore, Bedford, MA, USA). The membrane was preincubated in Tris-buffered saline (TBS) containing 0.01% Tween 20, 1% bovine serum albumin (BSA) for 1 h, and then incubated with anti-GAPDH monoclonal antibody (St. Louis, MO, USA), anti-phospho (Thr202/Tyr204)-specific p44/42 MAP kinase antibody (St. Louis, MO, USA), anti-p44/42 MAP kinase antibody (St. Louis, MO, USA), or anti-iNOS polyclonal antibodies overnight at 4 °C (diluted 1:2000). After incubation with horseradish peroxidase-conjugated or alkaline phosphatase-conjugated anti-rabbit/mouse IgG antibody, the immunoreactive bands were visualized with the enhanced chemiluminescence reagents (ECL, Amersham).

Acknowledgments

This work was supported by the Nation Science Council (NSC-96-2113-M-027-002-MY3). We are also grateful to the National Center for High-performance computing for the computer time and facilities.

Supplementary data

Supplementary data associated with this article can be found, in the online version, at doi:10.1016/j.bmc.2008.08.004.

References and notes

1. (a) Jialal, I.; Devaraj, S.; Venugopal, S. K. *Free Radical Res.* **2002**, *36*, 1331–1336; (b) Suryaprasad, A. G.; Prindiville, T. *Autoimmun. Rev.* **2003**, *2*, 346–357.
2. (a) Palmer, R. M.; Ashton, D. S.; Moncada, S. *Nature* **1988**, *333*, 664–666; (b) Duval, D. L.; Miller, D. R.; Collier, J.; Billings, R. E. *Mol. Pharmacol.* **1996**, *50*, 277–284.
3. Nakamura, E.; Isobe, H. *Acc. Chem. Res.* **2003**, *36*, 807.
4. Yang, J.; Alemany, L. B.; Driver, J.; Hartgerink, J. D.; Barron, A. R. *Chem. Eur. J.* **2007**, *13*, 2530–2545.
5. Da Ros, T.; Bergamin, M.; Vazquez, E.; Spalluto, G.; Baiti, B.; Moro, S.; Boutorine, A. S.; Prato, M. *Eur. J. Org. Chem.* **2002**, *3*, 405–413.
6. (a) Imahori, H.; Fukuzumi, S. *Adv. Funct. Mater.* **2004**, *14*, 525; (b) Guldi, D. M. *Pure Appl. Chem.* **2003**, *75*, 1069.
7. (a) de la Torre, M. D. L.; Rodrigues, A. G. P.; Tome, A. C.; Silva, A. M. S.; Cavaleiro, J. A. S. *Tetrahedron* **2004**, *60*, 3581; (b) del la Torre, M. D. L.; Marcorin, G. L.; Pirri, G.; Tome, A. C.; Silva, A. M. S.; Cavaleiro, J. A. S. *Tetrahedron Lett.* **2002**, *43*, 1689; (c) de la Torre, M. D. L.; Tome, A. C.; Silva, A. M.; Cavaleiro, J. A. S. *Tetrahedron Lett.* **2002**, *43*, 4617.
8. Krusic, P. J.; Wassermann, E.; Keizer, P. N.; Morton, J. R.; Preston, K. F. *Science* **1991**, *254*, 1183.
9. Kulkarni, R. G.; Achaiah, G.; Sastry, G. N. *Curr. Pharm. Des.* **2006**, *12*, 2437.

10. (a) Komatsu, W.; Ishihara, K.; Murata, M.; Saito, H.; Shinohara, K. *Free Radical Biol. Med.* **2003**, *34*, 1006; (b) Yamakoshi, Y.; Umexawa, N.; Ryu, A.; Arakane, K.; Miyata, N.; Goda, Y. J. *Am. Chem. Soc.* **2003**, *125*, 12803; (c) Gharbi, N.; Pressac, M.; Hadchouel, M.; Szwarc, H.; Wilson, S. R.; Moussa, F. *Nano Lett.* **2005**, *5*, 2578.
11. Huang, S. T.; Liao, J. S.; Fang, H. W.; Lin, C. M. *Bioorg. Med. Chem. Lett.* **2008**, *18*, 99–103.
12. (a) Satoh, M.; Matsuo, K.; Takanashi, Y.; Takayanagi, I. *Gen. Pharmacol.* **1995**, *26*, 1533; (b) Satoh, M.; Matsuo, K.; Kiriya, H.; Mashino, T.; Nagano, T.; Hirobe, M. *Eur. J. Pharmacol.* **1997**, *327*, 175; (c) Satoh, M.; Mashino, T.; Nagano, T.; Hirobe, M.; Takayanagi, I. *Fullerene Sci. Technol.* **2001**, *9*, 141.
13. Melchert, M.; List, A. *Int. J. Biochem. Cell Biol.* **2007**, *39*, 1489–1499.
14. Dumitru, C. D.; Ceci, J. D.; Tsatsanis, C.; Kontoyiannis, D.; Stamatakis, K.; Lin, J.-H.; Patriotis, C.; Jenkis, N. A.; Copeland, N. G.; Kollias, G. *Cell* **2000**, *103*, 1071–1083.
15. Hess, S.; Akermann, M. A.; Wnendt, S.; Zwingenberger, K.; Eger, K. *Bioorg. Med. Chem.* **2001**, *9*, 1279–1291.
16. Kordatos, K.; Da Ros, T.; Bosi, S.; Vázquez, E.; Bergamin, M.; Cusan, C.; Pellarini, F.; Véronique, T.; Benedetta, B.; Davide, P.; Georgakilas, V.; Giampiero, S.; Prato, M. J. *Org. Chem.* **2001**, *66*, 4915.
17. Wolleb, H.; Pfander, H. *Helv. Chim. Acta* **1986**, *69*, 1505.
18. (a) Hu, Z.; Guam, W.; Wang, W.; Huang, L.; Tang, X.; Xu, H.; Zhu, Z.; Xie, X.; Xing, H. *Carbon* **2008**, *46*, 99–109; (b) Partha, R.; Lackey, M.; Hirsch, A.; Casscells, W. S.; Conyers, J. L. J. *Nanobiotechnology* **2007**, *5*, 6.
19. Huang, S. T.; Tsai, H. D.; Kuo, H. S.; Yang, Y. P.; Peng, Y. C.; Lin, Y. L. *ChemBioChem* **2004**, *5*, 797.
20. Green, L. C.; Wagner, D. A.; Glogowski, J.; Skipper, P. L.; Wishnok, J. S. *Anal. Biochem.* **1982**, *126*, 131.
21. Cho, J. Y.; Park, J.; Yoo, E. S.; Yoshikawa, K.; Baik, K. U.; Lee, J. *Arch. Pharm. Res.* **1998**, *21*, 12.
22. Chang, Y. C.; Lee, F. W.; Chen, C. S.; Huang, S. T.; Tsai, S. H.; Huang, S. H.; Lin, C. M. *Free Radic. Biol. Med.* **2007**, *43*, 1541–1551.
23. Yang, J.; Wang, K.; Driver, J.; Yang, J.; Barron, A. R. *Org. Biomol. Chem.* **2007**, *5*, 260–266.